Journal of Alloys and Compounds, 201 (1993) 23–28
JALCOM 736

The microstructures and magnetic properties of some cast and annealed Pr–Fe–Cu–B alloys

G. J. Mycock[a], R. N. J. Faria[b] and I. R. Harris[b]*
[a]*Johnson Matthey, Rare Earth Products, Widnes, Cheshire (UK)*
[b]*School of Metallurgy and Materials, University of Birmingham, Edgbaston, Birmingham, B15 2TT (UK)*

(Received February 11, 1993)

Abstract

This paper reports the results of investigations of the microstructures and magnetic properties of some cast and annealed Pr–Fe–Cu–B alloys represented by the formulae, $Pr_xFe_{94.3-x}Cu_{2.0}B_{3.7}$, $Pr_{20.5}Fe_{75.8-x}Cu_xB_{3.7}$ and $Pr_{20.5}Fe_{77.5-x}Cu_{2.0}B_x$. Microstructural examination of these alloys showed that most of them exhibited $Pr_2Fe_{14}B$ plate-like grains with the *c*-axis perpendicular to the plate surface and there was *c*-axis alignment in the plane perpendicular to the predominant cooling direction. Scanning electron microscopy examination of the alloys showed that the copper was concentrated in the inter-crystalline regions and only trace quantities (<0.4at.%) of copper were detected in the $Pr_2Fe_{14}B$ phase. A eutectic mixture and a needle-like phase were observed in the inter-crystalline regions. The permanent magnet properties of the alloys, subject to various casting conditions and heat treatments, were investigated and enhanced properties were observed perpendicular to the predominant cooling direction. The largest $(BH)_{max}$ value (70 kJ m^{-3}) was achieved for the $Pr_{20.5}Fe_{73.8}Cu_{2.0}B_{3.7}$ alloy after annealing at 1000 °C for 5 h to remove the free iron. An improvement in the intrinsic coercivity of 73% was observed for this alloy on annealing for 3 h at 500 °C. Attempts have been made to correlate the permanent magnetic properties of the alloys with their corresponding microstructures.

1. Introduction

Fully dense Nd–Fe–B-type permanent magnets are manufactured usually by sintering pre-aligned and compacted powders. As there are a number of critical steps in this process involving reactive powdered material, attempts have been made to develop simpler, more cost-effective methods for the production of fully dense magnets. One such method is the production of magnets by the hot deformation of ingot material either by pressing [1–13], extrusion [14–18] or rolling [4, 19–21] at high temperatures (about 1000 °C). Shimoda *et al.* [1] showed that, in Pr–Fe–Cu–B alloys, significant permanent-magnet properties could be achieved even in the cast condition, and they identified an optimum composition of $Pr_{17}Fe_{76.5}Cu_{1.5}B_5$ for hot pressing. These and other studies showed that, in order to obtain good permanent-magnet properties on hot deformation, it is necessary to optimise the initial cast structure. This was reported to be a fine-grained columnar structure with the *c*-axis of the $Pr_2Fe_{14}B$ grains randomly distributed in the plane, perpendicular to the cooling direction. Chen and co-workers [7, 8] investigated the microstructures and magnetic properties of cast and hot-pressed $Pr_{19}Fe_{74.5}Cu_{1.5}B_5$ alloy, whereas Faria *et al.* [22] and Kwon *et al.* [9–12] studied similar properties in the alloy $Pr_{20.5}Fe_{73.8}Cu_2B_{3.7}$. Chen *et al.* [8] and Kwon *et al.* [11, 12] presented similar models in terms of $Pr_2Fe_{14}B$ crystal rotation to explain their experimental observations on hot-pressed magnets and the latter identified plate-like grains in their alloy with the *c*-axis perpendicular to the plate surface. This was a critical observation in view of the hot-pressing behaviour. Faria *et al.* [23] have produced high-coercivity sintered magnets using the $Pr_{20.5}Fe_{73.8}Cu_2B_{3.7}$ composition.

Scanning electron microscopy (SEM) and transmission electron microscopy (TEM) studies [9, 10, 13, 24] on the Pr–Fe–Cu–B alloys have shown that there is very little copper in the matrix $Pr_2Fe_{14}B$ phase and the grain-boundary regions consist of Pr-rich–PrCu-type eutectic mixture.

Kwon *et al.* [9, 10] indicated a higher Pr content for the intermetallic constituent of the eutectic but this is probably a result of electron-beam overlap with the neighbouring Pr-rich phase. These workers [9, 10] identified a needle-like phase in addition to the eutectic mixture with the composition $Pr_{32.3}Fe_{62.5}Cu_{4.1}B_{1.1}$ and the amount of this phase was found to increase on

*Author to whom correspondence should be addressed.

0925-8388/93/$6.00

annealing at 500 °C. A phase $Pr_{32.3}Fe_{62}Cu_{5.5}$ has been observed by Kajitani *et al.* [13] which is close to the composition reported by Kwon *et al.* [9, 10] and they also observed that this phase formed in the grain boundaries during heat treatment at around 500 °C. The phase was identified [13] as a tetragonal $Pr_6Fe_{13}Cu$ compound, space group I4/mcm.

The present paper reports the results of some further work on alloys at and around the $Pr_{20.5}Fe_{73.8}C_{2.0}B_{3.7}$ composition and was undertaken in order to optimise the composition with regard to the magnetic properties of the cast and annealed alloys. This is a necessary precursor to the production of hot-pressed magnets based on these compositions and also provides information on the possibility of producing orientated cast magnets from these alloys by appropriate mould design.

2. Materials and experimental methods

All the alloys studied in this work were prepared from a single batch of 99% praseodymium, 99.99% iron, 99.9% copper and commercial grade ferro-boron. The compositions of the various alloys are given by:

$Pr_xFe_{(94.3-x)}Cu_{2.0}B_{3.7}$, where $x = 19.5$, 20.5, 21.5;
$Pr_{20.5}Fe_{(77.5-x)}Cu_{2.0}B_x$, where $x = 3.2$, 3.7, 4.5, 5.2;
$Pr_{20.5}Fe_{(75.8-x)}Cu_xB_{3.7}$, where $x = 1.0$, 2.0, 3.0, 4.0, 5.0.

The raw materials were alloyed in a one-step operation by melting in an alumina crucible, using a vacuum induction furnace and a partial argon atmosphere. The maximum temperature, pouring temperature and dwell time were held constant for all the alloys and water-cooled copper moulds (maximum dimensions $100 \times 120 \times 8$ mm^3) were employed which gave rectangular, slab-shaped ingots. The cooling rates were increased by placing copper inserts into the mould thus decreasing the ingot thickness.

Rectangular blocks with dimensions about 10 mm × 10 mm × ingot thickness (representing approximately 1% of the ingot volume) were produced, usually from the central region of the ingot. In one case, however, wider sampling was employed, with samples from the ingot edge as well as from the middle of the ingot. Prior to the preparation of these blocks, the rough chill zone, adjacent to the mould wall, was ground away. All the samples were vacuum-annealed at 1000 °C for 5 h in order to remove the free iron and, in the case of three blocks, this was followed by a 3 h anneal at either 300, 400 or 500 °C. All the annealing treatments were terminated by a slow furnace cool to room temperature.

The microstructures of the alloys were examined in the polished and etched (15% nital) states, using a JOEL JXA-840A SEM and the various phases were analysed using energy dispersive X-ray analysis (EDX). A permeameter was used to measure the magnetic properties after the samples had been pulsed in a magnetic field of 6 T. These properties were measured perpendicular and parallel to the predominant cooling direction.

3. Results and discussion

3.1. Microstructural characterisation

The microstructure of a $Pr_{20.5}Fe_{73.8}Cu_{2.0}B_{3.7}$ alloy after annealing at 1000 °C for 5 h and cooling slowly to room temperature is shown in Fig. 1. The sample is shown in the as-polished condition and is viewed perpendicular to the predominant cooling direction. In this case, the top surfaces of the platelet-shaped $Pr_2Fe_{14}B$-type grains (A) can be seen (*c*-axis orientation according to Kwon *et al.* [10–12]) and, in the intercrystalline regions, there is a needle-like phase (B) and a eutectic mixture (C). The free iron observed in the cast material has been removed completely by this heat treatment. These observations are similar to those reported by Kwon *et al.* [9, 10] after a similar heat treatment. EDX measurements indicate that only trace quantities (<0.4at.%) of copper are present in the matrix grains and the eutectic mixture consists of predominantly praseodymium and a copper-rich phase (Pr + PrCu according to other workers who have examined the compositions $Pr_{17}Fe_{77.5}Cu_{1.5}B_4$ [24] and $Pr_{17}Fe_{76}Cu_{1.5}B_{5.5}$ [13]). The EDX studies also indicated regions which contain close to 100%Pr. The needle-like phase (B) was analysed to have a composition $Pr_{34}Fe_{62}Cu_4$ (neglecting the possible B content) and this is close to the composition identified by Kwon *et al.* [9, 10] and by Kajitani *et al.* [13]. If the specimens

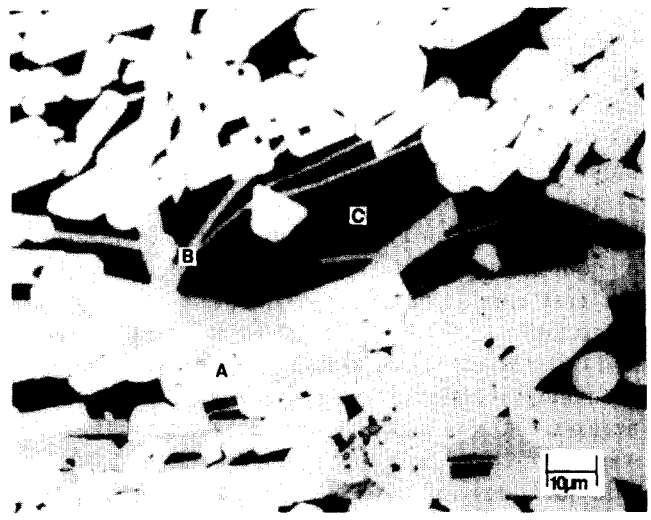

Fig. 1. The microstructure of the $Pr_{20.5}Fe_{73.8}Cu_{2.0}B_{3.7}$ alloy in the as-polished state, viewed perpendicular to the predominant cooling direction: (A) matrix phase, (B) "needle-like" phase, (C) eutectic mixture.

were etched in nital then this highlighted the crystal morphology but obscured the eutectic mixture in the inter-crystalline regions. Two other alloys with increased Cu content were also examined (namely, $Pr_{20.5}Fe_{72.8}Cu_{3.0}B_{3.7}$ and $Pr_{20.5}Fe_{71.8}Cu_{4.0}B_{3.7}$) and these exhibited a similar microstructure to that described above, apart from significantly reduced quantities of the needle-like phase.

Figure 2 shows another region of the $Pr_{20.5}Fe_{73.8}Cu_{2.0}B_{3.7}$ alloy after heat treatment, again perpendicular to the predominant cooling direction but now in the etched condition (nital). It can be seen that the alloy consists of small, well-isolated platelet-type grains, this time with the platelets viewed predominantly "edge-on" rather than on the top surface. The eutectic mixture is not visible in the etched condition.

Microstructural examination of the more B-rich compositions (4.5 and 5.2%B) showed that they exhibited a relatively large grain size compared with that of the $Pr_{20.5}Fe_{73.8}Cu_{2.0}B_{3.7}$ alloy and there was some evidence of crystal clusters giving poorer isolation of the individual crystallites, as shown in Fig. 3 for the $Pr_{20.5}Fe_{73.0}Cu_{2.0}B_{4.5}$ alloy.

3.2. *Magnetic characterisation*

The magnetic properties measured perpendicular to the predominant cooling direction of the heat treated samples (1000 °C for 5 h) are summarised in Tables 1, 2 and 3. The magnetic properties parallel to this direction have also been determined and, in all cases, much inferior properties have been obtained. Typically, a $Pr_{20.5}Fe_{73.8}Cu_{2.0}B_{3.7}$ alloy gave a remanence of only 57 mT, a coercivity of 195 KAm^{-1} and a $(BH)_{max}$ value of 0.52 KJm^{-3}. The second quadrant demagnetisation curve (C) for this alloy is shown in Fig. 4 together with those measured perpendicular to the predominant cooling direction, (A) and (B). This behaviour is typical of all the alloys studied in this work and the magnetic and microstructural observations indicate that the platelet $Pr_2Fe_{14}B$ crystals are growing within the tetragonal basal plane and along the predominant cooling direction, *i.e.*, perpendicular to the large face of the rectangular mould. This behaviour results in the alignment of the *c*-axes of the platelets in a plane at right angles to the

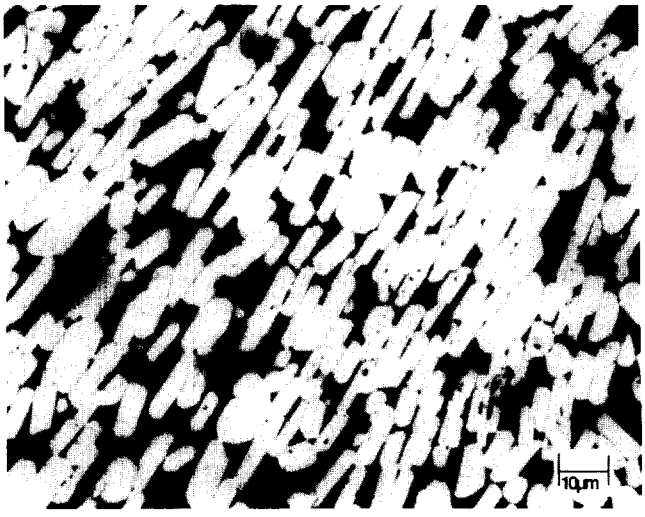

Fig. 2. The microstructure of the $Pr_{20.5}Fe_{73.8}Cu_{2.0}B_{3.7}$ alloy, viewed perpendicular to the predominant cooling direction, etched in 15% nital.

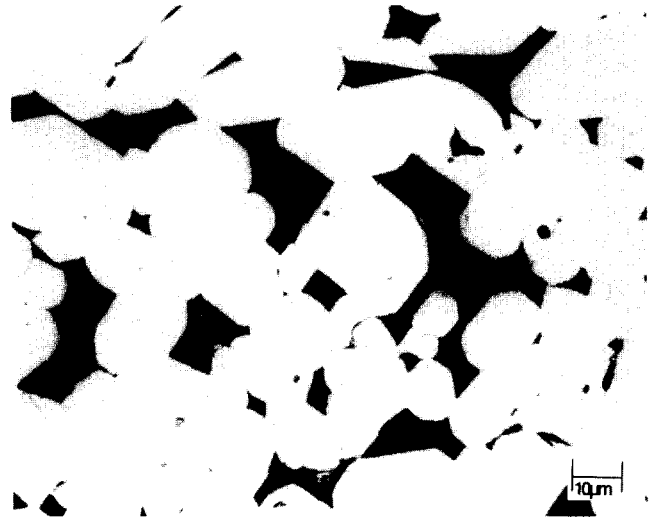

Fig. 3. The microstructure of the $Pr_{20.5}Fe_{73.0}Cu_{2.0}B_{4.5}$ alloy, viewed perpendicular to the predominant cooling direction, etched in 15% nital.

TABLE 1. Variation of magnetic properties with varying Pr content, for the composition $Pr_xFe_{(94.3-x)}Cu_{2.0}B_{3.7}$, measured perpendicular to the cooling direction

Value of x (at.%)	Coercivity (kAm^{-1}) ±5.0	Remanence (mT) ±10.0	Energy product (kJm^{-3}) ±1.0
19.5	109	261	5
20.5	553	641	70
21.5	719	568	57

TABLE 2. Variation of magnetic properties with varying B content, for the composition $Pr_{20.5}Fe_{(77.5-x)}Cu_{2.0}B_x$, measured perpendicular to the cooling direction

Value of x (at.%)	Coercivity (kAm^{-1}) ±5.0	Remanence (mT) ±10.0	Energy product (kJm^{-3}) ±1.0
3.2	88	597	54
3.7	553	641	70
4.5	173	395	16
5.2	206	396	18

TABLE 3. Variation of magnetic properties with varying Cu content, for the composition $Pr_{20.5}Fe_{(75.8-x)}Cu_xB_{3.7}$, measured perpendicular to the cooling direction

Value of x (at.%)	Coercivity (kAm^{-1}) ± 5.0	Remanence (mT) ± 10.0	Energy product (kJm^{-3}) ± 1.0
1.0	646	634	66
2.0	553	641	70
3.0	654	618	62
4.0	666	620	66
5.0	581	589	58

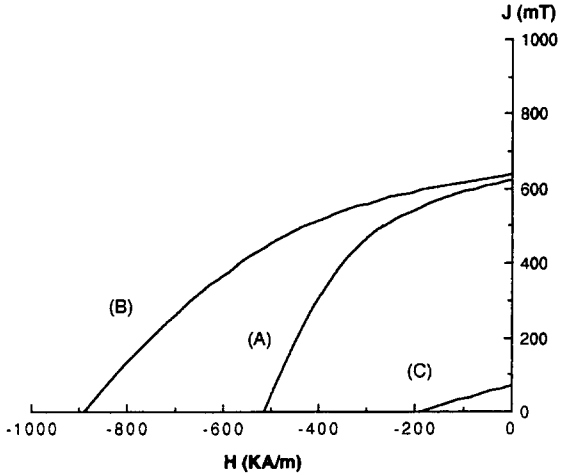

Fig. 4. Second quadrant hysteresis loop of the $Pr_{20.5}Fe_{73.8}Cu_{2.0}B_{3.7}$ alloy: (A) sample annealed at 1000 °C for 5 h, measured perpendicular to predominant cooling direction; (B) sample further annealed at 500 °C for 3 h, measured perpendicular to predominant cooling direction; (C) same treatment as (A), but measured parallel to the predominant cooling direction.

growth direction and the nature of this alignment will depend upon the nature of the heat flow within the mould during solidification.

If this interpretation is correct then, when viewed along the cooling direction, only the thin section of the platelet grains should be observable whereas, perpendicular to this direction, it should be possible to observe a range of cross-sections up to the full platelet surface as the c-axis rotates within this section. This is, in fact, in accordance with the present microstructural observations for the $Pr_{20.5}Fe_{73.8}Cu_{2.0}B_{3.7}$ alloy and is illustrated clearly in the ferrofluid pictures for this alloy shown in Figs. 5 and 6.

Table 1 shows that the 19.5%Pr alloy exhibits very poor magnetic properties, even in the favourable directions. Microstructural examination indicated that the $Pr_2Fe_{14}B$ grains were not well-isolated in this alloy. However, these drastic reductions in magnetic properties should be viewed with some caution until further trials can be carried out on this alloy. The best $(BH)_{max}$ value is observed for the $Pr_{20.5}Fe_{73.8}Cu_{2.0}B_{3.7}$ alloy and

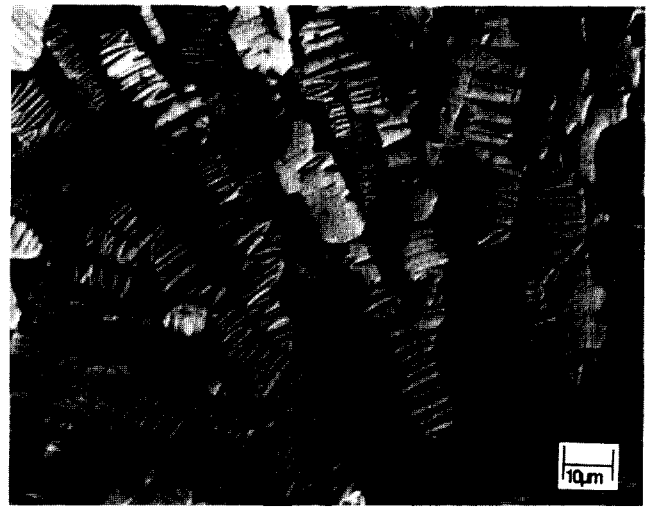

Fig. 5. Ferrofluid picture of the $Pr_{20.5}Fe_{73.8}Cu_{2.0}B_{3.7}$ alloy, viewed parallel to the predominant cooling direction showing that the c-axes of the plate-like matrix grains lie within the plane perpendicular to this direction.

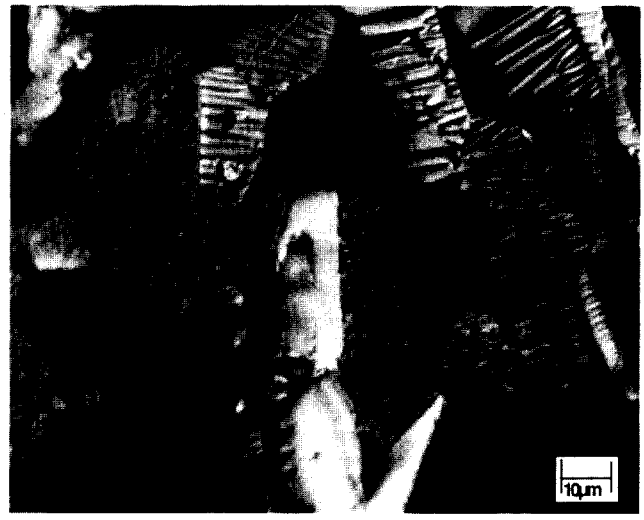

Fig. 6. Ferrofluid picture of the $Pr_{20.5}Fe_{73.8}Cu_{2.0}B_{3.7}$ alloy, viewed perpendicular to the predominant cooling direction showing that there is rotation of the platelet grains within this section.

this is also true for Tables 2 and 3. The poorer magnetic properties for the 4.5 and 5.2%B alloys could be the result of increased grain size and poorer magnetic isolation as indicated in Fig. 3. Table 3 shows that the magnetic properties are not particularly sensitive to the Cu content.

The present studies indicate that $Pr_{20.5}Fe_{73.8}Cu_{2.0}B_{3.7}$ represents the optimum composition within the range studied in this work. The alloy compositions investigated in this work are significantly more rare-earth-rich than the Pr–Fe–Cu–B alloys studied in earlier work by Shimoda *et al.* [1].

3.3. Variation in casting conditions

Two ingots with the optimum composition $Pr_{20.5}Fe_{73.8}Cu_{2.0}B_{3.7}$ were cast into narrower rectangular moulds with cavity widths of 6 and 4 mm (by inserting Cu plates). Because of the narrowness of the samples from these ingots it was not possible to use the permeameter to measure the magnetic properties parallel to the predominant cooling direction. However, at right angles to the cooling direction, both samples exhibited relatively high coercivities of 754 and 914 kAm^{-1} respectively together with corresponding remanence values of 605 and 596 mT respectively. The increased coercivities can be ascribed to a decreased mean grain size due to the increased cooling rate; and the decreased grain size has been confirmed by metallographic studies.

Six samples (dimensions $10\times10\times8$ mm^3) of the optimum composition alloy were cut from a rectangular ingot of overall dimensions ($100\times120\times8$ mm^3) from the edge (top, middle and bottom) and from a central region (top, middle and bottom). It might have been anticipated that samples from the edge of the ingot would have experienced a more complex cooling behaviour compared with that of samples from the central region and this would have influenced the *c*-axis orientation distribution of the $Pr_2Fe_{14}B$ crystals. However, the magnetic properties did not exhibit significant deviations from one another or from the results reported earlier.

3.4. Two-stage heat treatment

A number of previous studies have shown that annealing at about 500 °C results in a significant improvement in the coercivity of some hot deformed Pr–Fe–Cu–B alloys and Kwon *et al.* [10–12] and subsequently Kajitani *et al.* [13] have ascribed this improvement, partially at least, to an increase in the amount of the grain boundary $Pr_{32.3}Fe_{62.5}Cu_{4.1}B_{1.1}$ phase [10] (or $Pr_{32.3}Fe_{62}Cu_{5.5}$ [13] phase). In the present work, three samples from a heat-treated (1000 °C for 5 h) $Pr_{20.5}Fe_{73.8}Cu_{2.0}B_{3.7}$ alloy were shown to exhibit very similar magnetic properties perpendicular to the predominant cooling direction. One sample was then heat-treated at 300 °C, one at 400 °C and the third at 500 °C, all for 3 h (a similar time to that employed in previous studies). The magnetic properties were re-determined after these treatments and the results are summarised in Table 4. It can be seen that after annealing at 300 and 400 °C, only small, barely significant changes were observed in the remanence and coercivity, whereas after annealing at 500 °C, there was a small increase in the remanence and a dramatic improvement in the coercivity of some 73%. These changes in the magnetic properties are shown in Fig. 4 and the improved coercivity might be due to an increase in the amount of the needle-like phase at the grain boundaries. This phase is known to form at temperatures around 500 °C and the magnetic data shown in Table 4 could indicate either that this phase does not form at the lower annealing temperatures or that longer annealing times are required.

TABLE 4. Magnetic properties of an alloy, $Pr_{20.5}Fe_{73.8}Cu_{2.0}B_{3.7}$, after treatment at 1000 °C for 2 h, then further annealing at various temperatures for 3 h. Measurements are taken perpendicular to the cooling direction. The values in parentheses are the percentage changes after annealing at the various temperatures shown

Annealing temp. (°C)	Coercivity (kAm^{-1}) ±5.0	Remanence (mT) ±10.0	Energy product (kJm^{-3}) ±1.0
300	507(−2.2%)	655(+1.2%)	69(+4.5%)
400	502(−2.1)	655(+0.2%)	70(+14.6%)
500	896(+73.3%)	643(5.3%)	70(+14.6%)

4. Conclusion

(1) The alloy with the best magnetic properties in the cast/annealed state exhibit "plate-like" $Pr_2Fe_{14}B$ crystals with the *c*-axis perpendicular to the plate surface. The crystals are arranged so that the *c*-axes lie within a plane perpendicular to the predominant cooling direction and the best magnetic properties are obtained in this plane.

(2) Of the compositions studied in this work, the best overall magnetic properties are exhibited by the alloy $Pr_{20.5}Fe_{73.8}Cu_{2.8}B_{3.7}$.

(3) Small changes in the Pr and B concentration result in significant losses in the magnetic properties and metallographic studies indicate that these losses could be the result of an increase in grain size and poorer magnetic isolation of the $Pr_2Fe_{14}B$ grains.

(4) The magnetic properties are not very sensitive to small changes in the Cu concentrations.

(5) The present results indicate that there is scope for further improvements of the magnetic properties of cast and annealed $Pr_{20.5}Fe_{73.8}Cu_{2.0}B_{3.7}$ alloy with appropriate changes in mould design and casting procedures.

(6) Annealing at 500 °C results in a very significant improvement in the coercivity of the cast/annealed magnets and this could be related to an increase in the amount of the needle-like phase at the grain boundaries.

Acknowledgments

The authors wish to acknowledge the support of Johnson Matthey, Rare Earth Products, for G. J. Mycock

and of CNEN (*Comissao Nacional de Energia Nuclear*) and CNPq (*Conselho Nacional de Desenvolvimento Cientifico e Tecnologico*), for R.N.J. Faria. Thanks are also due to SERC, CEAM and EURAM for their support of the general research programme of which this forms a part.

References

1 T. Shimoda, K. Akioka, O. Kobayashi and T. Yamagami, *J. Appl. Phys., 64* (10) (1988) 5290.
2 T. Shimoda, K. Akioka, O. Kobayashi and T. Yamagami, *J. de Physique, C8,* (12) (1988) 49.
3 T. Shimoda, K. Akioka, O. Kobayashi and T. Yamagami, *IEEE Trans. Magn., 25* (1989) 4099.
4 T. Shimoda, K. Akioka, O. Kobayashi and T. Yamagami, *Proc. 10th Int. Workshop on RE Magnets and Their Applications,* Kyoto, Japan, 1989, p. 389.
5 T. Shimoda, K. Akioka, O. Kobayashi and T. Yamagami, *J. Appl. Phys., 69* (8) (1991) 5829.
6 Y. Luo and N. Zhang, *Proc. 10th Int. Workshop on RE Magnets and Their Applications,* Kyoto, Japan, 1989, p. 275.
7 Z. Chen, F. Xie, Z. Shi, L. Wang and H. Fu, *J. Appl. Phys., 70* (5) (1991) 2868.
8 Z. Chen, Z. Shi, L. Wang and H. Fu, *J. Appl. Phys., 71* (6) (1992) 2799.
9 H. W. Kwon, P. Bowen and I. R. Harris, *J. Appl. Phys., 70* (10) (1991) 6357.
10 H. W. Kwon, P. Bowen and I. R. Harris, *J. Alloys Comp., 182* (1992) 233.
11 H. W. Kwon, P. Bowen and I. R. Harris, *Proc. 12th Int. Workshop on RE Magnets and Their Applications,* Canberra, Australia, 1992, p. 705.
12 H. W. Kwon, P. Bowen and I. R. Harris, *J. Alloys Comp., 189* (1992) 131.
13 T. Kajitani, K. Nagayama and T. Umeda, *Proc. 12th Int. Workshop on RE Magnets and Their Applications,* Canberra, Australia, 1992, p. 574.
14 W. Ervens, *CEAM Report,* Elsevier Applied Science, 1989, p. 655.
15 J. P. Nozières and R. Perrier de la Bâthie, *IEEE Trans. Mag., 25* (1989) 4117.
16 J. P. Nozières and R. Perrier de la Bâthie, *J. Phys. (Paris), 49* (C8) (1988) 667.
17 J. P. Nozières, R. Perrier de la Bâthie and J. Gavinet, *J. Magn. Magn. Mater., 80* (1989) 88.
18 J. P. Nozières, R. Perrier de la Bâthie and D. W. Taylor, *CEAM Report,* Elsevier Applied Science, 1989, p. 659.
19 T. Ohki, T. Yuri, M. Miyagawa, Y. Takahashi, C. Yoshida, S. Kambe, M. Higashi and K. Hayama, *Proc. 10th Int. Workshop on RE Magnets and Their Applications,* Kyoto, Japan, 1989, p. 399.
20 T. Mukai and H. Sakamoto, *Appl. Phys. Lett., 54* (16) (1989) 1597.
21 T. Shimoda, K. Akioka, O. Kobayashi, T. Tamagami and A. Arai, *Proc. 11th Int. Workshop on RE Magnets and Their Applications,* Pittsburgh, 1990, p. 17.
22 R. N. Faria, J. S. Abell and I. R. Harris, *J. Appl. Phys., 70* (10) (1991) 6104.
23 R. N. Faria, J. S. Abell and I. R. Harris, *J. Alloys Comp., 177* (1992) 311.
24 J. Fidler and J. Bernadi, *J. Appl. Phys., 70* (10) (1991) 6456.